Metal Carbonyl Bond Strengths in $Fe(CO)_n^-$ and $Ni(CO)_n^-$

L. S. Sunderlin, Dingneng Wang,† and Robert R. Squires*

Contribution from the Department of Chemistry, Purdue University, West Lafayette, Indiana 47907. *Received August 1, 1991*

Abstract: Energy-resolved collision-induced dissociation of $Fe(CO)_n^-$ (n = 1-4) and $Ni(CO)_n^-$ (n = 2, 3) is used to determine the metal-carbonyl bond energies (kcal/mol) $D[(CO)_3Fe^-CO]$ = 41.7 ± 2.5, $D[(CO)_2Fe^-CO]$ = 42.4 ± 3.5, $D[(CO)Fe^-CO]$ = 35.7 ± 3.5, $D[Fe^-CO]$ = 33.7 ± 3.5, $D[(CO)_2Ni^-CO]$ = 38.5 ± 2.3, and $D[(CO)Ni^-CO]$ = 43.4 ± 5.8. The sum of the iron-carbonyl bond strengths is within error limits of the value derived from previous experimental results. Combining the nickel data with the known energy for loss of all CO ligands from $Ni(CO)_3^-$ gives $D[Ni^-CO]$ = 32.4 ± 5.8 kcal/mol. The bond energies in the anions can be used with literature electron affinities to give bond energies (kcal/mol) for the neutral metal carbonyls, $D[(CO)_3Fe-CO]$ = 27.9 ± 8.8, $D[(CO)_2Fe-CO]$ = 29.1 ± 5.8, $D[(CO)Fe-CO]$ = 36.7 ± 3.5, $D[Fe-CO]$ = 8.1 ± 3.5, $D[(CO)_2Ni-CO]$ = 28.3 ± 2.3, $D[(CO)Ni-CO]$ = 47.1 ± 5.8, and $D[Ni-CO]$ = 40.5 ± 5.8. Estimates of the ionization potentials of neutral $Ni(CO)_n$ and $Fe(CO)_n$ fragments are also derived. These results are compared to previous experimental and theoretical estimates of the M-CO bond strengths. Consideration of the electronic structures and electron binding energies of the $M(CO)_n^-$ ions suggests that the dissociations occur adiabatically, with little or no effects of electron detachment on the measured dissociation thresholds.

Introduction

The rapid growth of organometallic chemistry has led to an increased demand for reliable thermochemical data pertaining to transition-metal organometallic compounds, particularly metal-ligand bond energies.[1] Binary transition-metal carbonyls are among the earliest known[2] and most commonly encountered organometallic compounds.[3] Moreover, metal carbonyl fragments are ubiquitous components of other organometallic compounds and larger metal clusters,[4] and they are frequently invoked as active species in homogeneous catalytic cycles.[3,5,6] Accordingly, the strengths of metal-carbonyl bonds are of paramount concern in organometallic chemistry. For many coordinatively saturated homoleptic metal carbonyl complexes the average M-CO bond strengths are known from calorimetric measurements.[7,8] However, a knowledge of the sequential, rather than average, bond strengths is necessary for an understanding of the individual properties of coordinatively unsaturated metal carbonyl fragments, as well as for delineating periodic and homologous trends in M-CO bonding. Reliable theoretical descriptions of metal carbonyl complexes are now becoming available that allow predictions to be made of sequential M-CO bond strengths,[9,10] further emphasizing the need for accurate experimental measurements of these quantities.

A variety of experimental methods have been used to determine metal-carbonyl bond strengths. The first M-CO bond energy in stable, coordinatively saturated (usually neutral) metal carbonyls is traditionally estimated from the measured Arrhenius activation energies for ligand substitution reactions in solution[11,12] or the gas phase[12,13] that proceed by dissociative mechanisms. A more recent solution-based method is photoacoustic calorimetry.[14] Gas-phase techniques are usually required for evaluating M-CO bond energies in smaller, highly coordinatively unsaturated metal carbonyl fragments. For example, neutral iron carbonyl bond strengths have been estimated through modeling of time-of-flight distributions of products of $Fe(CO)_5$ photodissociation.[15] The first two metal-carbonyl bond strengths in $Cr(CO)_6$ have been determined through modeling of the recombination kinetics of $Cr(CO)_4$ and $Cr(CO)_5$ with CO,[16] and other metal-carbonyl bond strengths have been estimated by modeling the competing dissociation and collisional stabilization of excited metal carbonyls.[17,18] Other spectroscopic studies on saturated[19] and unsaturated metal carbonyls[20,21] have provided significant kinetic and structural information, but relatively little thermochemistry. Bond strengths have been determined for *cationic* metal carbonyl fragments by measuring electron impact appearance potentials for $M(CO)_n^+$ from neutral metal carbonyls,[22] photoionization[23] and photoelectron-photoion coincidence spectra,[24] kinetic energy release distributions of metastable manganese carbonyl cations,[25] and energy-resolved collision-induced dissociation of $Fe(CO)_n^+$.[26] For

† Current address: Chemical Conversion Research Branch, National Renewable Energy Laboratory, 1617 Cole Blvd., Golden, CO 80401.

(1) Simões, J. A. M.; Beauchamp, J. L. *Chem. Rev.* **1990**, *90*, 629-688.
(2) Mond, L.; Langer, C.; Quincke, F. *J. Chem. Soc.* **1890**, 749. Mond, L.; Langer, C. *J. Chem. Soc.* **1891**, 1090. Berthelot, M. *Compt. Rend.* **1891**, *112*, 1343.
(3) Cotton, F. A.; Wilkinson, G. *Advanced Inorganic Chemistry*, 5th ed.; Wiley: New York, 1988. Collman, J. P.; Hegedus, L. S.; Norton, J. R.; Finke, R. G. *Principles and Applications of Organotransition Metal Chemistry*; University Science Books: Mill Valley, CA, 1987. Kochi, J. K. *Organometallic Mechanisms and Catalysis*; Academic Press: New York, 1978.
(4) Elian, M.; Hoffmann, R. *Inorg. Chem.* **1975**, *14*, 1058-1076. Hoffmann, R. *Angew. Chem., Int. Ed. Engl.* **1982**, *21*, 711-724.
(5) Tolman, C. A. *Chem. Soc. Rev.* **1972**, *1*, 337-353. Casey, C. P.; Cyr, C. R. *J. Am. Chem. Soc.* **1973**, *95*, 2248-2253. Mitchener, J. C.; Wrighton, M. S. *J. Am. Chem. Soc.* **1981**, *103*, 975-977. Whetten, R. L.; Fu, K.; Grant, E. R. *J. Chem. Phys.* **1982**, *77*, 3769-3770. Whetten, R. L.; Fu, K.; Grant, E. R. *J. Am. Chem. Soc.* **1982**, *104*, 4270-4272.
(6) Weitz, E. *J. Phys. Chem.* **1987**, *91*, 3945-3953.
(7) Connor, J. A. *Top. Curr. Chem.* **1977**, *71*, 71-110.
(8) Pilcher, G.; Skinner, H. A. In *The Chemistry of the Metal-Carbon Bond*; Hartley, F. R., Patai, S., Eds.; Wiley: New York, 1982; Chapter 2.
(9) Barnes, L. A.; Rosi, M.; Bauschlicher, C. W. *J. Chem. Phys.* **1991**, *94*, 2031-2039. See references therein for previous calculations on $Fe(CO)_n$.
(10) Ziegler, T.; Tschinke, V.; Ursenbach, C. *J. Am. Chem. Soc.* **1987**, *109*, 4825-4837.
(11) Siefert, E. E.; Angelici, R. J. *Organomet. Chem.* **1967**, *8*, 374-376.
(12) Day, J. P.; Basolo, F.; Pearson, R. G. *J. Am. Chem. Soc.* **1968**, *90*, 6927-6933.
(13) Lewis, K. E.; Golden, D. M.; Smith, G. P. *J. Am. Chem. Soc.* **1984**, *106*, 3905-3912.
(14) Bernstein, M.; Simon, J. D.; Peters, K. S. *Chem. Phys. Lett.* **1983**, *100*, 241-244. Morse, J. M.; Parker, G. H.; Burkey, T. J. *Organometallics* **1989**, *8*, 2471-2474.
(15) Venkataraman, B. K.; Bandukwalla, G.; Zhang, Z.; Vernon, M. *J. Chem. Phys.* **1989**, *90*, 5510-5526.
(16) Fletcher, T. R.; Rosenfield, R. N. *J. Am. Chem. Soc.* **1988**, *110*, 2097-2101.
(17) Rayner, D. Y.; Ishikawa, Y.; Brown, C. E.; Hackett, P. A. *J. Chem. Phys.* **1991**, *94*, 5471-5480.
(18) Ishikawa, Y.; Hackett, P. A.; Rayner, D. M. *J. Am. Chem. Soc.* **1987**, *109*, 6644-6650. Ishikawa, Y.; Brown, C. E.; Hackett, P. A.; Rayner, D. M. *J. Phys. Chem.* **1990**, *94*, 2404-2413.
(19) Waller, I. M.; Hepburn, J. W. *J. Chem. Phys.* **1988**, *88*, 6658-6669. Schlenker, F. J.; Bouchard, F.; Waller, I. M.; Hepburn, J. W. *J. Chem. Phys.* **1990**, *93*, 7110-7118. Ray, U.; Brandow, S. L.; Bandukwalla, G.; Venkataraman, B. K.; Zhang, Z.; Vernon, M. *J. Chem. Phys.* **1988**, *89*, 4092-4101.
(20) Breeze, P. A.; Burdett, J. K.; Turner, J. J. *Inorg. Chem.* **1981**, *20*, 3369-3378.
(21) Burdett, J. K. *Coord. Chem. Rev.* **1978**, *27*, 1-58 and references cited therein. Poliakoff, M.; Weitz, E. *Adv. Organomet. Chem.* **1987**, *25*, 277-316. Weiller, B. H.; Grant, E. R. In *Gas Phase Inorganic Chemistry*; Russell, D. H., Ed.; Plenum Press: New York, 1989.
(22) Examples for $Fe(CO)_5$ and $Ni(CO)_4$ include: Winters, R. E.; Kiser, R. W. *Inorg. Chem.* **1964**, *3*, 699-702. Foffani, A.; Pignataro, S.; Cantone, B.; Grasso, F. *Z. Phys. Chem.* **1965**, *45*, 79-88. Bidinosti, D. R.; McIntyre, N. S. *Can. J. Chem.* **1967**, *45*, 641-648. Junk, G. A.; Svec, H. J. *Z. Naturforsch.* **1968**, *23b*, 1-9.
(23) Distefano, G. *J. Res. Natl. Bur. Stand.* **1970**, *74A*, 233-238.
(24) Norwood, K.; Ali, A.; Flesch, G. D.; Ng, C. Y. *J. Am. Chem. Soc.* **1990**, *112*, 7502-7508.

0002-7863/92/1514-2788$03.00/0

anionic metal carbonyl fragments, measurements of the appearance energy (AE) of chromium,[27] molybdenum,[27] tungsten,[27] iron,[27,28] and nickel[28] carbonyl anions are currently the only direct source of individual bond strengths.

In recent reports from this laboratory,[29,30] we have described measurements of collision-induced dissociation (CID) threshold energies using a flowing afterglow-triple quadrupole apparatus and the use of these data in deriving thermodynamic properties for organic and inorganic ions and neutral molecules. In this study, we present our measurements of the bond strengths in $Fe(CO)_n^-$ (n = 1–4) and $Ni(CO)_n^-$ (n = 1–3) ions and a derivation of the M–CO bond energies in the corresponding neutral fragments. We have also combined the neutral M–CO bond strengths with literature values for the corresponding cations to obtain estimates of the ionization potentials of $Fe(CO)_n$ and $Ni(CO)_n$ fragments. Possible sources of error in the derived thermochemistry are discussed. Comparisons with the currently available measurements and theoretical predictions of the sequential and average bond strengths in both the ionic and neutral metal carbonyls are also made. The M–CO bond strengths and $M(CO)_n$ heats of formation obtained in the present study are combined with relevant results in the literature to derive additional new thermochemical data for organometallic compounds.

Experimental Section

All experiments were performed with a flowing afterglow-triple quadrupole apparatus described previously.[31] The operating conditions in the 7.3 cm i.d. × 100 cm flow tube were P(He) = 0.40 Torr, F(He) = 190 cm^3(STP)/s, and T = 298 K. The metal carbonyl anions were formed by electron impact (EI) or in a dc discharge, with $Fe(CO)_5$ or $Ni(CO)_4$ added at the upstream end of the flow reactor. With the dc discharge source, a ca. 5:1 He:Ar mixture is used instead of pure He. Using EI, $Fe(CO)_4^-$, $Fe(CO)_3^-$, and $Ni(CO)_3^-$ could be made in sufficient abundance to perform CID experiments. Larger quantities of $Fe(CO)_3^-$, as well as $Fe(CO)_2^-$, $FeCO^-$, and $Ni(CO)_2^-$, are obtained using the dc discharge source.[32]

For some of the experiments involving the dc discharge source, the concentrations of smaller fragment ions such as $Fe(CO)^-$ were increased by imposing a drift field immediately after the ion source to induce CID in the flow tube. This involves leaving the flow tube at ground and floating the ion source and a small tube covered with a 95% transmittance Ni mesh inserted inside the flow tube to ca. −100 V. This exposes the ions to an ≈100-V potential drop over the distance of a few centimeters, thereby inducing collisional activation.

Ions are thermalized by ca. 10^5 collisions with the helium bath gas. The possibility that He is an inefficient cooling gas was tested by adding 4–7 mTorr of isobutane to the flow. Since isobutane has a large number of vibrational degrees of freedom and a much higher polarizability than He, it should provide effective cooling of hot ions.[33] Addition of isobutane had no measurable effect on the results for the $Fe(CO)_4^-$ and $Ni(CO)_3^-$ systems. This indicates that isobutane does not increase cooling, strongly suggesting that helium alone is sufficient to thermalize the ions. Experiments using the different ion sources give the same results within the experimental precision.

Ions in the flow tube are gently extracted through a 1-mm orifice into a region of differential pumping and then focused into an Extrel triple quadrupole mass analyzer. The desired reactant ion is selected with the first quadrupole and injected into the radio frequency-only, gas-tight central quadrupole (Q2) with an axial kinetic energy determined by the Q2-pole offset voltage. Argon or xenon is maintained in Q2 at a pressure of ≤5 × 10^{-2} mTorr. Fragment ions resulting from single or multiple ligand loss are efficiently contained in Q2 and extracted by a low voltage exit lens into the third quadrupole, which is maintained at an attractive voltage with respect to the variable Q2 pole offset voltage. Ion detection is carried out with a conversion dynode and an electron multiplier operating in pulse-counting mode.

CID Threshold Measurement and Analysis. Detailed accounts of the data collection procedures and analysis method for CID threshold energy measurements have been provided recently.[29] The axial kinetic energy of the mass-selected reactant ion is scanned, while the intensity of the CID fragment ion formed in Q2 under single-collision conditions is monitored. The center-of-mass collision energy E_{CM} for the system is given by $E_{CM} = E_{lab}[m/(M + m)]$, where E_{lab} is the nominal laboratory energy and M and m represent the masses of the reactant ion and neutral target, respectively. The energy axis origin is verified by retarding potential analysis, and the reactant ion kinetic energy distribution is found to have a near-Gaussian shape with a full width at half-maximum (FWHM) of 0.5–2 eV (laboratory).

Absolute cross sections are calculated by use of $\sigma_p = I_p/INl$, where σ_p is the cross section for a particular product, I_p is the intensity of the product (counts/s), N is the number density of the neutral reagent, l is the effective path length for reaction (measured to be 24 ± 4 cm by comparison with the known cross section[34] for the reaction of Ar^+ with D_2 to form ArD^+), and I is the intensity of the reactant ion beam. This is accurate as long as the extent of conversion of reactant ions to products remains low (less than ca. 5%). The neutral reagent pressure in Q2 (≤0.05 mTorr) is low enough to ensure predominantly single collision conditions. Under these conditions, less than 4% of the ions react.

Phase incoherence between the quadrupoles of the triple quadrupole mass analyzer causes oscillations in the apparent intensity of the reactant ion, but not the CID product ions, as the Q2 pole offset voltage is scanned.[35] For this reason, the intensity of the reactant ion beam is estimated to be equal to the maximum transmitted intensity in the region of the thresholds for dissociation. The absolute cross sections may also be in error because of different collection or detection efficiencies for the reactant and product ions. These two factors are the main source of inaccuracies in the absolute cross sections, which have an estimated uncertainty of a factor of 2. We therefore show normalized cross sections in the appearance plots, and note the estimated cross sections in the text. Relative cross sections should be more reliable (ca. ±50%).

The activation energy for the dissociation may be deconvoluted from the ion appearance curve by means of a fitting procedure based on the assumed model function given by eq 1, where $I(E)$ is the intensity of the

$$I(E) = I_0[(E - E_T)^n/E^m] \quad (1)$$

product ion at center-of-mass collision energy E, E_T is the desired threshold energy, I_0 is a scaling factor, and n and m are adjustable parameters. On the basis of previous theoretical[36,37] and experimental[29,38] results for CID and other reactive collisions, m is held to 1. Optimization is carried out by an iterative procedure in which n, I_0, and E_T are varied to minimize the deviations between the experimental and calculated appearance curves in the steeply rising portion of the threshold region.[39] The region near and below the threshold is not fit because of tailing in the data that is attributed to translational excitation of the ions in the first quadrupole or to internal excitation due to collisions outside the interaction region. Attempts to fit that region of the observed excitation function lead to unreasonably high values for n and thresholds near 0. Convoluted into the fit are the reactant ion kinetic energy distribution approximated by a Gaussian function with a 2-eV (laboratory) FWHM and a Doppler broadening function developed by Chantry to account for the random thermal motion of the neutral target.[40] The CID threshold, E_T, derived in this way is considered to correspond to a thermal activation energy for production of room-temperature (298 K) products from thermalized, room-temperature reactants. Therefore, the reaction threshold is taken to be the 298 K bond energy. In order to convert E_T to a bond dissociation enthalpy term for use in deriving heats of forma-

(25) Dearden, D. V.; Hayashibara, K.; Beauchamp, J. L.; Kirchner, N. J.; van Koppen, P. A. M.; Bowers, M. T. *J. Am. Chem. Soc.* **1989**, *111*, 2401–2409.

(26) Schultz, R. H.; Crellin, K. C.; Armentrout, P. B. *J. Am. Chem. Soc.* **1991**, *113*, 8590–8601.

(27) Pignataro, S.; Foffani, A.; Grasso, F.; Cantone, B. *Z. Phys. Chem. (Frankfurt)* **1965**, *47*, 106–113.

(28) Compton, R. N.; Stockdale, J. A. D. *Int. J. Mass Spectrom. Ion Phys.* **1976**, *22*, 47–55.

(29) Graul, S. T.; Squires, R. R. *J. Am. Chem. Soc.* **1990**, *112*, 2517–2529. Paulino, J. A.; Squires, R. R. *J. Am. Chem. Soc.* **1991**, *113*, 5573–5580.

(30) Marinelli, P. J.; Squires, R. R. *J. Am. Chem. Soc.* **1989**, *111*, 4101–4103. Workman, D. B.; Squires, R. R. *Inorg. Chem.* **1988**, *27*, 1846–1848. Hajdasz, D. J.; Squires, R. R. *J. Chem. Soc., Chem. Commun.* **1988**, 1212–1214. Wenthold, P. G.; Paulino, J. A.; Squires, R. R. *J. Am. Chem. Soc.* **1991**, *113*, 7414–7415.

(31) Graul, S. T.; Squires, R. R. *Mass Spectrom. Rev.* **1988**, *7*, 263–358.

(32) The discharge conditions were typically 1000 V and 4 mA passing between copper electrodes 5 mm apart. Greater production of highly unsaturated metal carbonyl anions with increasing emission current at the ion source was noted previously in ref 63.

(33) Ferguson, E. E. *Adv. At. Mol. Phys.* **1989**, *25*, 61–81.

(34) Ervin, K. M.; Armentrout, P. B. *J. Chem. Phys.* **1985**, *83*, 166–189.

(35) Dawson, P. H., Ed. *Quadrupole Mass Spectrometry and Its Applications*; Elsevier: New York, 1976. Miller, P. E.; Bonner Denton, M. *Int. J. Mass Spectrom. Ion Processes* **1986**, *72*, 223.

(36) Chesnavich, W. J.; Bowers, M. T. *J. Phys. Chem.* **1979**, *83*, 900–905.

(37) Rebick, C.; Levine, R. D. *J. Chem. Phys.* **1973**, *58*, 3942–3952.

(38) Sunderlin, L. S.; Armentrout, P. B. *Int. J. Mass Spectrom. Ion Processes* **1989**, *94*, 149–177 and references cited therein.

(39) The data is analyzed using the CRUNCH program written by Prof. P. B. Armentrout et al.

(40) Chantry, P. J. *J. Chem. Phys.* **1971**, *55*, 2746–2759.

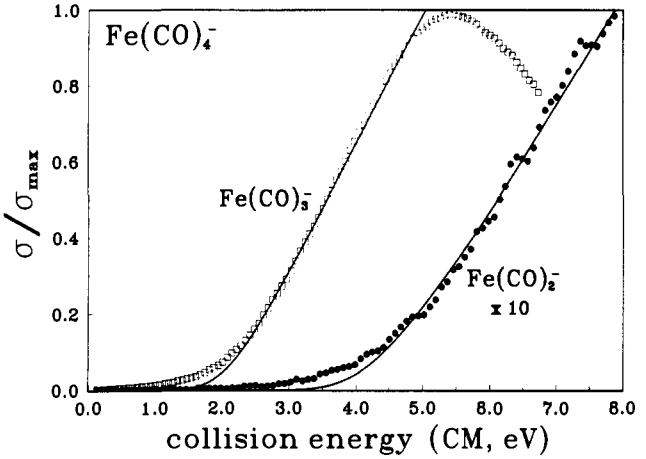

Figure 1. Appearance curves for products from CID of $Fe(CO)_4^-$ as a function of kinetic energy. The solid lines are model appearance curves calculated using eq 1 and convoluted as discussed in the text. The eq 1 parameters are n = 1.71, E_T = 1.84 for $Fe(CO)_3^-$ and n = 1.75, E_T = 3.71 for $Fe(CO)_2^-$.

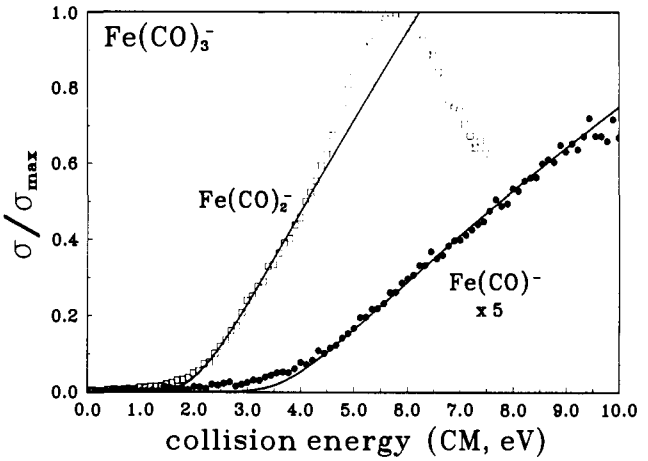

Figure 2. Appearance curves for products from CID of $Fe(CO)_3^-$ as a function of kinetic energy. The solid lines are model appearance curves calculated using eq 1 and convoluted as discussed in the text. The eq 1 parameters are n = 1.77, E_T = 1.77 for $Fe(CO)_2^-$ and n = 1.60, E_T = 3.37 for $Fe(CO)^-$.

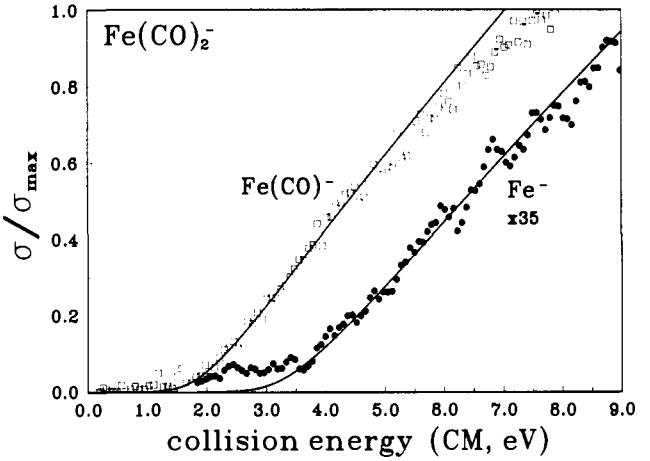

Figure 3. Appearance curves for products from CID of $Fe(CO)_2^-$ as a function of kinetic energy. The solid lines are model appearance curves calculated using eq 1 and convoluted as discussed in the text. The eq 1 parameters are n = 1.72, E_T = 1.56 for $Fe(CO)^-$ and n = 1.7, E_T = 2.95 for Fe^-.

tion, an expansion work factor ΔnRT is added, where Δn is the change in the number of molecules for the reaction. (At 298 K, RT = 0.6 kcal/mol.)

Schultz et al. have explicitly included the reactant ion vibrational energy distribution when fitting CID data.[26] The vibrational frequencies of the metal carbonyl anions are not completely known, but the known[41] frequencies of $Ni(CO)_4$ are a reasonable approximation for those in $Fe(CO)_4^-$. At 298 K, $Ni(CO)_4$ contains an average of 4.9 kcal/mol of vibrational energy. The smaller reactant anions have fewer vibrational modes and less internal energy, and their vibrational frequencies can be approximated as subsets of the $Ni(CO)_4$ frequencies. For the metal carbonyls used in this work, which have many low-frequency modes, the energy distribution is strongly peaked around the average energy, such that internal energy introduces significant broadening in the dissociation cross section very near or below the threshold, but not at higher energies. Fits taking into account the vibrational energy distribution[42] are indistinguishable from those which do not include the distribution over the energy range where the fit is optimized. The two methods give thresholds within 0.01 eV of each other.[43] A more significant effect (0.09–0.12 eV) was found in the analysis of CID of $Fe(CO)_n^+$, where the data was fit to lower energies.[26]

In this study, both argon and xenon are used as collision gases. Argon has the advantage of being essentially monoisotopic, and its lower mass means that broadening due to the ion energy distribution is smaller in the center-of-mass frame. Xenon is often more efficient at inducing dissociation near the threshold[26,44] and gives 20–32% less Doppler broadening than Ar for the present reactions. The xenon results are therefore useful as a check on the experiments using an argon target gas. In these experiments, xenon is treated as a monoisotopic gas of the average atomic weight, 131.3 amu.

Reagents were obtained from commercial sources: He (99.995%) and Ar (99.995%) from Airco, Xe (99.999%) and isobutane (99%) from Matheson, $Fe(CO)_5$ (99.5%) from Alfa, and $Ni(CO)_4$ from Strem.

Results

Iron. The products observed from CID of $Fe(CO)_4^-$ with argon and xenon (rare gases, Rg) correspond to loss of one to three carbonyl ligands, reactions 2–4. Relative cross sections for reactions 2–4 are plotted as a function of center-of-mass collision energy in Figure 1 (Rg = Ar). The respective maximum cross sections for reactions 2–4 in the energy range plotted are estimated to be 15, 1.5, and 0.2 Å^2 (Rg = Ar) and 16.2, 2.9, and 0.3 Å^2 (Rg = Xe). Loss of one CO ligand is therefore the dominant process, with multiple dissociation channels showing successively higher thresholds and significantly lower yields.

$$Fe(CO)_4^- \xrightarrow{Rg} \begin{cases} Fe(CO)_3^- + CO & (2) \\ Fe(CO)_2^- + 2CO & (3) \\ Fe(CO)^- + 3CO & (4) \end{cases}$$

The relative cross sections for reactions 5 and 6 are plotted as a function of kinetic energy in Figure 2 (Rg = Ar). Cross sections for reactions 5 and 6 are estimated to be 16 and 2.4 Å^2 (Rg = Ar). No other reactions were observed within the sensitivity of the instrument.

$$Fe(CO)_3^- \xrightarrow{Rg} \begin{cases} Fe(CO)_2^- + CO & (5) \\ Fe(CO)^- + 2CO & (6) \end{cases}$$

The relative cross sections for reactions 7 and 8 are plotted as a function of kinetic energy in Figure 3 (Rg = Ar). The maximum cross section for these reactions are estimated to be 7.3 and 0.2 Å^2, respectively.

$$Fe(CO)_2^- \xrightarrow{Rg} \begin{cases} Fe(CO)^- + CO & (7) \\ Fe^- + 2CO & (8) \end{cases}$$

The relative cross section for reaction 9 is plotted as a function of kinetic energy in Figure 4 (Rg = Ar). The maximum cross section for reaction 9 is estimated to be 6.2 Å^2.

$$Fe(CO)^- \xrightarrow{Rg} Fe^- + CO \quad (9)$$

(41) Bouquet, G.; Bigorgne, M. *Spectrochim. Acta* **1971**, *27A*, 139–149.
(42) The fitting procedure is similar to that described in ref 26, and the Whitten–Rabinovitch formula for the density of vibrational states is used: Whitten, G. Z.; Rabinovitch, B. S. *J. Chem. Phys.* **1963**, *38*, 2466–2473.
(43) Since the measured CID thresholds are presumed to correspond to 298 K reactants and products, the 298 K energy content of the reactant ion must be subtracted from thresholds derived when the internal energy content is explicitly included in the fit.
(44) Aristov, N.; Armentrout, P. B. *J. Phys. Chem.* **1986**, *90*, 5135–5140.

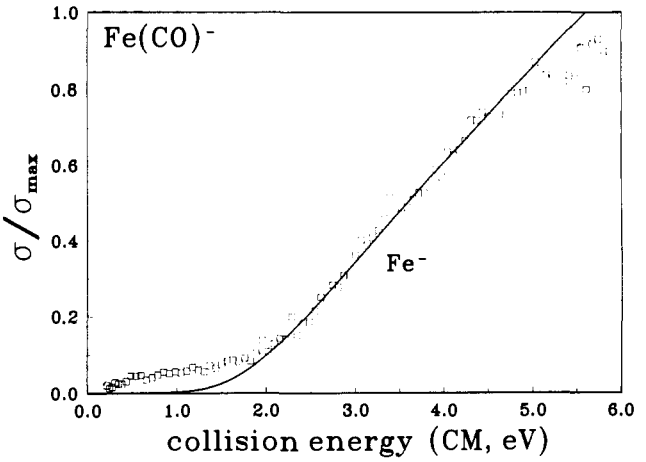

Figure 4. Appearance curve for production of Fe^- from CID of $Fe(CO)^-$ as a function of kinetic energy. The solid line is a model appearance curve calculated using eq 1 and convoluted as discussed in the text. The eq 1 parameters are $n = 1.72$ and $E_T = 1.48$.

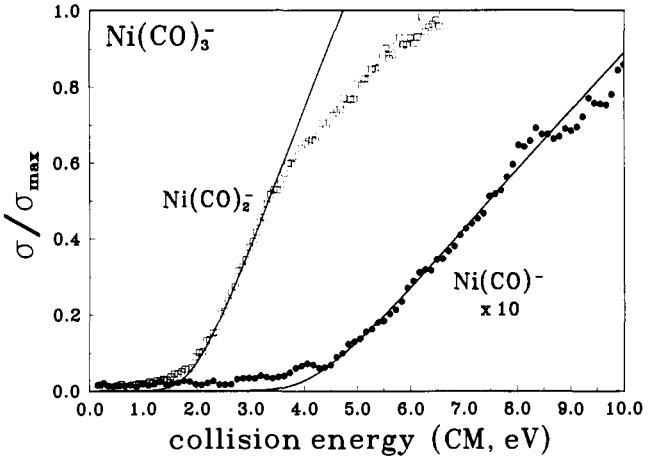

Figure 5. Appearance curve products from CID of $Ni(CO)_3^-$ as a function of kinetic energy. The solid lines are model appearance curves calculated using eq 1 and convoluted as discussed in the text. The eq 1 parameters are $n = 1.72$, $E_T = 1.69$ for $Ni(CO)_2^-$ and $n = 1.70$, $E_T = 3.70$ for $Ni(CO)^-$.

Nickel. Relative cross sections for the products observed from CID of $Ni(CO)_3^-$ with argon are plotted as a function of kinetic energy in Figure 5. As in the iron systems, these reactions correspond to loss of one or two carbonyl ligands, reactions 10 and 11. The maximum cross sections for reactions 10 and 11

$$Ni(CO)_3^- \xrightarrow{Rg} Ni(CO)_2^- + CO \quad (10)$$

$$Ni(CO)_3^- \xrightarrow{Rg} Ni(CO)^- + 2CO \quad (11)$$

in the energy range plotted are 8.0 and 0.7 Å^2 (Rg = Ar) and 7.6 and 1.1 Å^2 (Rg = Xe). A trace of Ni^- was also observed, with insufficient intensity for analysis.

The relative cross section for reaction 12 is plotted as a function of kinetic energy in Figure 6 (Rg = Ar). The maximum cross section for this reaction in the energy range plotted is 3.9 Å^2. A trace of Ni^- was also observed, with insufficient intensity for analysis.

$$Ni(CO)_2^- \xrightarrow{Rg} Ni(CO)^- + CO \quad (12)$$

The maximum total cross sections for all of the reactions examined in this work are in the range of 6–16 Å^2. For comparison, total cross sections for CID of $Fe(CO)_n^+$ ($n = 2$–4) with Xe are in the 13–35-Å^2 range. In the present data, loss of $n + 1$ carbonyl ligands is a factor of 6–12 less efficient than loss of n carbonyl ligands for all systems where multiple ligand dissociations are possible, with the exception of the anomalously low cross section for reaction 8, which is discussed below. Similar effects are also generally evident in the $Fe(CO)_n^+$ CID data[26] and are apparent

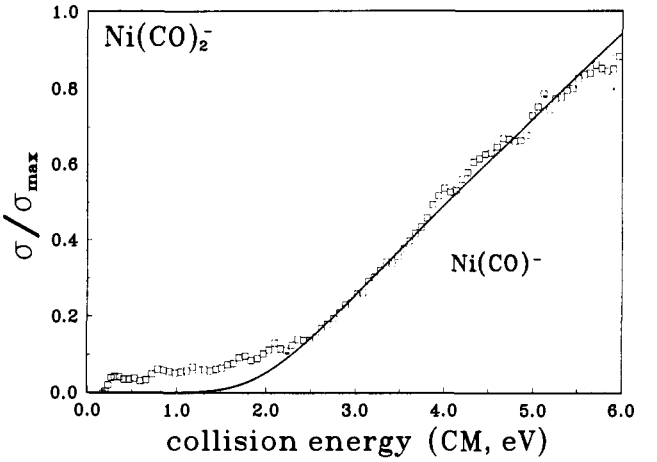

Figure 6. Appearance curves for production of $Ni(CO)^-$ from CID of $Ni(CO)_2^-$ as a function of kinetic energy. The solid line is a model appearance curve calculated using eq 1 and convoluted as discussed in the text. The eq 1 parameters are $n = 1.70$ and $E_T = 1.70$.

Table I. Fitting Parameters[a]

reacn no.	Rg	E_T (eV)	n
2	Ar	1.84 ± 0.10	1.71 ± 0.16
2	Xe	1.78 ± 0.12	1.76 ± 0.19
3	Ar	3.71 ± 0.10	1.75 ± 0.16
3	Xe	3.81 ± 0.48	1.7 ± 0.2 (held)
5	Ar	1.77 ± 0.15	1.77 ± 0.28
6	Ar	3.37 ± 0.30	1.60 ± 0.13
7	Ar	1.56 ± 0.06	1.72 ± 0.18
8	Ar	2.95 ± 0.26	1.7 ± 0.2 (held)
9	Ar	1.48 ± 0.17	1.72 ± 0.15
10	Ar	1.69 ± 0.10	1.72 ± 0.25
10	Xe	1.63 ± 0.14	1.7 ± 0.2 (held)
11	Ar	3.70 ± 0.29	1.7 ± 0.2 (held)
11	Xe	3.75 ± 0.28	1.7 ± 0.2 (held)
12	Ar	1.70 ± 0.24	1.7 ± 0.2 (held)

[a] Optimal fitting parameters for eq 1 with $m = 1$.

in the electron impact appearance energy measurements for the iron carbonyl anions.[28]

Threshold Determinations. The optimized fitting parameters used with eq 1 are listed in Table I, and some of the corresponding fits are shown in Figures 1–6. The error limits listed are standard deviations for the parameters optimized individually for multiple data sets. The standard deviation of E_T is a good estimate for the accuracy of the derived bond dissociation energies. The precision of the data, as measured by the variation in the thresholds of individual data sets with n held constant, is typically better than 0.05 eV.

In order to test the effect of the mass of the neutral target, both Ar and Xe were used as target gases for some reactions. The cross section energy dependences in the steeply rising portion of the excitation function were the same within experimental error for these reactions. The Xe data has more of a tail at low energies and is therefore more difficult to fit with precision. For the systems studied here, there are no systematic differences between thresholds derived using the two different targets.

Reactions 2 (Rg = Ar and Xe), 3, 5–7, 9, and 10 (Rg = Ar) all optimized with values of n from 1.60 to 1.77. This suggests that $n = 1.7$ is applicable to most or all of the reactions studied. Data for the remaining reactions are not sufficiently robust to allow n to optimize, as different data sets gave widely differing values for n and E_T. We therefore held n to 1.7 ± 0.2 (optimizing E_T for $n = 1.5$, 1.7, and 1.9) for these reactions. This variation in n is expected to give realistic error limits for the thresholds. For all reactions, $n = 1.7$ provides a good fit to the data. The results of these fits are also listed in Table I.

E_T for reaction 2 is equivalent to the measured bond energy $D[(CO)_3Fe^-–CO]$, provided there are no barriers to dissociation in excess of the endothermicity (see Discussion below). The values for Rg = Ar (1.84 ± 0.10 eV) and Rg = Xe (1.78 ± 0.12 eV)

can be averaged to give $D[(CO)_3Fe^-–CO] = 1.81 \pm 0.11$ eV (41.7 ± 2.5 kcal/mol). E_T for reaction 3 (Rg = Ar), 3.71 ± 0.10 eV corresponds to the energy needed to remove two carbonyl ligands, leading to $D[(CO)_2Fe^-–CO] = 3.71 - 1.81 = 1.90 \pm 0.15$ eV. The threshold for reaction 3 with Rg = Xe (3.81 ± 0.48 eV) is consistent with this result but not of sufficient precision to be included in the final determination of thermochemistry. The threshold for reaction 5 (1.77 ± 0.15 eV) is also a measurement of $D[(CO)_2Fe^-–CO]$. The two determinations combine to give $D[(CO)_2Fe^-–CO] = 1.84 \pm 0.15$ eV (42.4 ± 3.5 kcal/mol), where the uncertainty is estimated. The threshold for reaction 7 gives $D[(CO)Fe^-–CO] = 1.56 \pm 0.06$ eV, while $D[(CO)_2Fe^-–CO] = 1.84 \pm 0.15$ eV can be subtracted from the threshold for reaction 6 (3.37 ± 0.30 eV) to give $D[(CO)Fe^-–CO] = 1.53 \pm 0.34$ eV. These two determinations are in good agreement and can be combined to give $D[(CO)Fe^-–CO] = 1.55 \pm 0.15$ eV (35.7 ± 3.5 kcal/mol), where the uncertainty is again estimated. Finally, the difference between the threshold for reaction 8 and $D[(CO)Fe^-–CO]$ (1.40 ± 0.30 eV) and the threshold for reaction 9 (1.51 ± 0.10 eV) can be averaged to give $D[Fe^-–CO] = 1.46 \pm 0.15$ eV (33.7 ± 3.5 kcal/mol), where the uncertainty is again estimated.

Results for reaction 10 reported in Table I give thresholds of 1.69 ± 0.10 eV (Rg = Ar) and 1.63 ± 0.14 eV (Rg = Xe). These combine to give $D[(CO)_2Ni^-–CO] = 1.66 \pm 0.10$ eV (38.3 ± 2.3 kcal/mol), where the argon results dominate the final average. Results for reaction 11 yield $D[(CO)Ni^-–2CO] = 3.70 \pm 0.29$ eV (Rg = Ar) and 3.75 ± 0.28 eV (Rg = Xe). $D[(CO)Ni^-–2CO] - D[(CO)_2Ni^-–CO]$ then gives $D[(CO)Ni^-–CO] = 2.04 \pm 0.31$ eV (Ar) or 2.09 ± 0.30 eV (Xe). The threshold for reaction 12 (1.70 ± 0.24 eV) is a direct measurement of $D[(CO)Ni^-–CO]$. These results can be averaged to give $D[(CO)Ni^-–CO] = 1.88 \pm 0.25$ eV (43.4 ± 5.8 kcal/mol), where the uncertainty is estimated.

Ligand Exchange Reactions. The measured threshold energies formally represent upper limits to the bond dissociation energies, since there could be barriers to dissociation in excess of the overall reaction endothermicity. However, if there is no barrier for the *reverse* process (i.e. addition of CO to a metal carbonyl anion), then the measured dissociation activation energies become equal to the reaction endothermicities. McDonald and Bianchina have examined in detail the reactions of $Fe(CO)_3^-$ with ^{13}CO in a flowing afterglow at 298 K.[45] Both addition and $^{13}CO/^{12}CO$ exchange occur under thermal conditions with nonnegligible efficiencies ($k_{obs}/k_{coll} = 0.24$). These results have been qualitatively confirmed in the present work, and similar reactivity is also observed for $Fe(CO)_2^-$. The reaction of $Fe(CO)_3^-$ with ^{13}CO in the collision cell of the triple quadrupole analyzer shows efficient exchange at low collision energy with an apparent cross section that decreases with increasing collision energy—behavior characteristic of a reaction with no activation energy. These observations indicate that there is no significant barrier to addition of CO to $Fe(CO)_2^-$ and $Fe(CO)_3^-$. This indicates that the thresholds for loss of CO from $Fe(CO)_3^-$ and $Fe(CO)_4^-$ are equal to the corresponding bond energies, assuming that the bound species formed by addition of CO to the metal carbonyls are in fact the ground-state adducts and not long-lived excited states of different spin (see Discussion below). Insufficient quantities of $Fe(CO)^-$, Fe^-, and $Ni(CO)_n^-$ (n = 0–2) could be made for analogous experiments.

Discussion

Electron Detachment. It is important to consider whether electron detachment competes effectively with ligand dissociation in these experiments. Efficient electron detachment could cause a competitive shift[46] in the thresholds by suppressing the cross sections for ligand loss. Photodetachment does occur for $Fe(CO)_n^-$ (n = 0–4)[47] and $Ni(CO)_n^-$ (n = 0–3)[48] in the gas phase and for $Fe(CO)_4^-$ in a low-temperature matrix.[20] However, photodissociation occurs for $Fe(CO)_3^-$,[49] $Ni(CO)_3^-$,[50] and other metal carbonyl anions,[50] and is the dominant process for $Fe(CO)_4^-$ upon irradiation with visible light.[51] Electron detachment cannot be observed directly in the present experiment, since the quadrupole collision chamber does not trap electrons.

One indirect test for electron detachment is to compare the measured dissociation thresholds with the known electron binding energies of the anions. For example, the threshold for reaction 2 is ca. 1.8 eV, while the electron affinity of $Fe(CO)_4$ is 2.4 eV. Thus, electron detachment should not occur at the dissociation threshold. No change in the $Fe(CO)_3^-$ appearance curve is apparent in the vicinity of 2.4 eV, suggesting that electron detachment does not significantly affect the observed dissociation cross section at these energies.

Another test is to compare the overall CID cross sections for the anions to those for CID of similar cations, where electron detachment cannot occur. The overall cross sections for the $Fe(CO)_n^-$ ions are somewhat smaller than for those in the $Fe(CO)_n^+$ systems.[26] This is probably due at least in part to the fact that the anion bond strengths are in general higher than the cation bond strengths. It has also been previously noted[52] that CID of $Fe(CO)_4^-$ and $Cr(CO)_5^-$ results in systematically lower yields for loss of more than two CO ligands compared to CID of the corresponding cations. This is confirmed by comparison of the recent $Fe(CO)_n^+$ cross-section measurements[26] to the present data. We interpret this to mean that significant electron detachment does occur at energies near the threshold for loss of *three* carbonyl ligands, but does not significantly affect the cross sections (and therefore the threshold determinations) for the first *one* or *two* carbonyl losses.

An exception to this is the anomalously low cross section for reaction 8, 0.2 Å^2. The fact that the cross section is about an order of magnitude lower than that for the 2CO loss channels from other iron carbonyl anions, even though the bonds being broken are weaker, suggests that another reaction channel may be competing. Since the electron affinity of Fe, 0.15 eV, is much lower than that of the iron carbonyls (Table IV), significant electron detachment from Fe^- may be occurring in this instance in the same energy range as loss of two carbonyls. Nevertheless, the cross section for this reaction has a typical shape, and the threshold is consistent with the other available data. We therefore include results for reaction 8 in the final thermochemical analysis.

A further test for possible electron detachment is to measure the energy dependence of the total cross section. The sum of the cross sections for all products in a CID reaction typically rises or remains roughly constant beyond a certain energy. The total cross sections for CID of iron carbonyl cations, for instance, are nearly constant in the 3–10-eV range.[26] A drop in the sum of the observed ligand dissociation channels may reflect electron detachment, the products of which are not observed. In the electron impact appearance energy (AE) measurements on $Fe(CO)_5$ and $Ni(CO)_4$,[28] the measured total cross section for dissociation declines rapidly with increasing energy after an initial rise, such that the total intensity of anionic products at 8 eV is a factor of ≥5000 less than at 1 eV. This indicates that electron detachment is the primary decay process for the transient $[Fe(CO)_5^-]^*$ intermediate formed in the electron impact experiment (i.e. the electron is usually scattered without reaction). In contrast, the total signal intensity for CID in the $Fe(CO)_4^-$ + Ar system peaks at 6-eV CM and is only 25% smaller at 13 eV. Such a small effect could be due to changes in fragment ion collection efficiency at different energies or to a change in the reaction cross section, as well as to electron detachment. This again suggests that electron de-

(45) McDonald, R. N.; Bianchina, E. J. *Organometallics* **1991**, *10*, 1274–1278.
(46) Lifshitz, C.; Long, F. A. *J. Chem. Phys.* **1964**, *41*, 2468–2471.
(47) Engelking, P. C.; Lineberger, W. C. *J. Am. Chem. Soc.* **1979**, *101*, 5569–5573.
(48) Stevens, A. E.; Feigerle, C. S.; Lineberger, W. C. *J. Am. Chem. Soc.* **1982**, *104*, 5026–5031.
(49) Rynard, C. M.; Brauman, J. I. *Inorg. Chem.* **1980**, *19*, 3544–3545.
(50) Dunbar, R. C.; Hutchinson, B. B. *J. Am. Chem. Soc.* **1974**, *96*, 3816–3820.
(51) Richardson, J. H.; Stephenson, L. M.; Brauman, J. I. *J. Am. Chem. Soc.* **1974**, *96*, 3671–3673.
(52) Wysocki, V. H.; Kenttämaa, H. I.; Cooks, R. G. *J. Phys. Chem.* **1988**, *92*, 6465–6469.

Table II. Iron Carbonyl Bond Strengths

bond	bond strength (kcal/mol) lit.	this work
$(CO)_3Fe^-$–CO	27.7[a]	41.7 ± 2.5
$(CO)_2Fe^-$–CO	46 ± 5[b]	42.4 ± 3.5
	52[c]	
(CO)Fe^-–CO	23 ± 7[b]	35.7 ± 3.5
	51[c]	
Fe^-–CO	46 ± 7[b]	33.7 ± 3.5
$(CO)_4$Fe–CO	41.5 ± 2[d]	
	58 ± 12[e]	
	42.5 ± 1.2[f]	
	16 ± 7[g]	
	23.9[i]	
	44.2[j]	
$(CO)_3$Fe–CO	5 ± 9[e]	27.9 ± 8.8
	10[h]	
	31[i]	
$(CO)_2$Fe–CO	32 ± 7[e]	29.1 ± 5.8
	25[h]	
	25[i]	
(CO)Fe–CO	23 ± 7[e]	36.7 ± 3.5
	51[c,e]	
	>27[h]	
	22[i]	
Fe–CO	23 ± 7[e]	8.1 ± 3.5
	<39[h]	
	5[i]	
$(CO)_4Fe^+$–CO	26.8 ± 0.9[k]	
$(CO)_3Fe^+$–CO	24.7 ± 1.4[k]	
$(CO)_2Fe^+$–CO	15.9 ± 1.2[k]	
(CO)Fe^+–CO	36.1 ± 1.8[k]	
Fe^+–CO	36.6 ± 1.8[k]	

[a] Calculated using eq 13. [b] Data from ref 28 with appearance energies assiged in ref 47. [c] Reference 27. Reproducibility of appearance energies stated to be 0.1–0.5 eV (2–12 kcal/mol). [d] Reference 13. [e] Reference 47. [f] Reference 11. This is a condensed phase result not used in this work because of possible solvent effects. [g] Pignataro, S.; Lossing, F. P. *J. Organomet. Chem.* **1968**, *11*, 571–576. [h] Reference 15. [i] Reference 9. [j] Reference 10. [k] Reference 26.

tachment is not the dominant reaction in the threshold region of the reactions analyzed in this work.

Comparison to Literature. Some previous experimental data for the metal carbonyl anions are available for comparison to the present results. In addition, the bond strengths in the anions can be converted to bond strengths in the neutral metal carbonyl fragments, as described below. These can be compared to a wider variety of experimental and theoretical determinations of $Fe(CO)_n$ and $Ni(CO)_n$ bond energies.

Iron Carbonyl. The two previous studies of iron carbonyl anion thermochemistry by Pignataro et al.[27] and Compton and Stockdale (CS)[28] both involve measurements of the appearance energies for production of $Fe(CO)_n^-$ fragments upon electron bombardment of $Fe(CO)_5$. Although ref 27 gives threshold values, ref 28 does not. These values have been estimated by Engelking and Lineberger (EL).[47] The differences in the literature AEs for each successive $M(CO)_n^-$ fragmentation can be used to derive metal–carbonyl bond strengths by use of eq 13. These results are

$$D[(CO)_nM^-–CO] = AE[M(CO)_n^-] - AE[M(CO)_{n+1}^-] \quad (13)$$

listed in Table II. Equation 13 is not valid when dissociative electron detachment is significantly exothermic, because in this case the $M(CO)_{n+1}^-$ appearance curve will simply correspond to the ion transmission function of the instrument, not the energetics of the reaction. When dissociative electron capture is exothermic, only a lower limit on the bond strength can be derived. CS suggested[47] that $D[(CO)_4Fe–CO] \approx EA[Fe(CO)_4]$; more recent data given in Tables II and IV indicate that this is not the case. Thus, $D[(CO)_3Fe^-–CO]$ derived by Engelking and Lineberger from the ion appearance curves reported by Compton and Stockdale is too low. For $D[(CO)_2Fe^-–CO]$, the EL results agree reasonably well with the present data. For $D[(CO)Fe^-–CO]$, the 35.7 ± 3.5 kcal/mol value derived in the present work lies halfway between the 23 ± 7 kcal/mol value derived by EL from the CS data and the 51 kcal/mol value from the Pignataro et al. data. In contrast, the present value for $D[Fe^-–CO]$, 33.7 ± 3.5 kcal/mol, is lower than the EL/CS literature value, 46 ± 7 kcal/mol. The sum of the last two bond strengths, $D[Fe^-–2CO]$, is 69.4 kcal/mol using the present results and 69 kcal/mol using the EL/CS results. Since the EL values are derived by comparing the differences between thresholds for successive ligand losses, the fact that the bond strengths derived by EL differ from the present values by −13 kcal/mol for $D[(CO)Fe^-–CO]$ and +12 kcal/mol for $D[Fe^-–CO]$ is most simply explained if the threshold for appearance of $Fe(CO)^-$ estimated by EL from the CS data is too low by ca. 12 kcal/mol (0.5 eV).

Table III. Nickel Carbonyl Bond Strengths

bond	bond energy (kcal/mol) lit.	this work
$(CO)_2Ni^-$–CO	23 ± 9[a]	38.5 ± 2.3
(CO)Ni^-–CO	51 ± 14[a]	43.4 ± 5.8
Ni^-–CO	21 ± 14[a]	32.4 ± 5.8
	21.2[b]	
$(CO)_3$Ni–CO	21.5 ± 0.4[c]	
	25 ± 2[d]	
	29.8[e]	
	25.3[f]	
$(CO)_2$Ni–CO	13 ± 10[d]	28.3 ± 2.3
	34.6[e]	
(CO)Ni–CO	54 ± 15[d]	47.1 ± 5.8
	42.6[e]	
Ni–CO	29 ± 15[d]	40.5 ± 5.8
	34.5[e]	
$(CO)_3Ni^+$–CO	10.4 ± 0.5[g]	
$(CO)_2Ni^+$–CO	30.7 ± 2.3[g]	
(CO)Ni^+–CO	35.7 ± 3.3[g]	
Ni^+–CO	48.4 ± 3.3[g]	

[a] Data from ref 28 with appearance energies assigned in ref 48. [b] Reference 55. [c] Reference 12. [d] Reference 48. [e] Reference 56. [f] Reference 10. [g] Reference 23.

The bond strength sum $D[Fe^-–4CO]$ can be calculated using eq 14 and the literature thermochemistry in Table III. The result is $D[Fe^-–4CO] = 147.8 \pm 7.6$ kcal/mol. The sum of the met-

$$D[Fe^-–4CO] = -\Delta H_f[Fe(CO)_5] + \Delta H_f(Fe^-) + 5\Delta H_f(CO) - D[(CO)_4Fe–CO] + EA[Fe(CO)_4] - 5kT \quad (14)$$

al–carbonyl bond strengths in $Fe(CO)_4^-$ measured here is 153.6 ± 6.5 kcal/mol, giving a difference of 6 ± 10 kcal/mol. Thus, the two results are within error limits of each other. The discrepancy suggests either that $EA[Fe(CO)_4]$ is at the upper end of the 2.4 ± 0.3 eV range or that the bond strengths measured here are high by an average of 1–2 kcal/mol.

It is possible to calculate $D[(CO)_3Fe^-–CO]$ using eq 15, literature thermochemistry in Table III, and $AE[Fe(CO)_3^-] = 0.55$ eV[27] or ca. 0.6 eV.[28] The literature AEs both give $D[(CO)_3Fe^-–CO] \approx 28$ kcal/mol, somewhat lower than the value obtained in this work. This is also consistent with $EA[Fe(CO)_4]$ being at the high end of the 2.4 ± 0.3 eV range. Alternatively, if the value for $D[(CO)_3Fe^-–CO]$ in the present work is too high, it would explain why the sum of the four bond strengths is high.

$$D[(CO)_3Fe^-–CO] = AE[Fe(CO)_3^-] - D[(CO)_4Fe–CO] + EA[Fe(CO)_4] \quad (15)$$

The anion thermochemistry can be combined with the known electron affinities (EAs) of neutral iron carbonyls[47] to give bond strengths for the neutral species using eq 16.[53] In some cases

$$D[(CO)_nM–CO] = D[(CO)_nM^-–CO] + EA[M(CO)_n] - EA[M(CO)_{n+1}] \quad (16)$$

this results in increased uncertainties because the error limits for the anion bond strength and two EAs all contribute to the un-

(53) This equation strictly applies to bond strengths at 0 K. It applies at 298 K if the difference between the heat capacities of $[M(CO)_n^- + M(CO)_{n+1}]$ and $[M(CO)_{n+1}^- + M(CO)_n]$ is negligible, which should hold true for these systems.

Table IV. Literature Thermochemistry

quantity	value[a]	quantity	value[a]
$\Delta H_f(Fe^-)$	96.1 ± 0.2	$\Delta H_f(Ni^-)$	76.0 ± 0.7
$\Delta H_f[Fe(CO)_5]$	−173 ± 2	$\Delta H_f[Ni(CO)_4]$	−143 ± 1
$EA[Fe(CO)_4]$	2.4 ± 0.3[b]	$EA[Ni(CO)_3]$	1.077 ± 0.013[d]
$EA[Fe(CO)_3]$	1.8 ± 0.2[b]	$EA[Ni(CO)_2]$	0.643 ± 0.014[d]
$EA[Fe(CO)_2]$	1.22 ± 0.02[b]	EA[Ni(CO)]	0.804 ± 0.012[d]
EA[Fe(CO)]	1.26 ± 0.02[b]	EA[Ni]	1.157 ± 0.010[c]
EA[Fe]	0.151 ± 0.003[c]	$\Delta H_f(CO)$	−26.42

[a] Data from (unless otherwise noted): Lias, S. G.; Bartmess, J. E.; Liebman, J. F.; Holmes, J. L.; Levin, R. D.; Mallard, W. G. *J. Phys. Chem. Ref. Data* **1988**, *17*, Suppl. 1. Heats of formation are in kcal/mol at 298 K; EAs are in eV and are defined at 0 K. [b] Reference 47. [c] Reference 61. [d] Reference 48.

certainty in the neutral bond strength. The results are given in Table II, along with literature values for the neutral bond strengths. These values correlate with the anion bond strengths such that there is good agreement between this study and the results of EL on the magnitude of $D[(CO)_2Fe-CO]$, but poor agreement on the other iron carbonyl bond strengths. The thermochemical estimates[15] derived by Venkataraman et al. from modeling of time-of-flight distributions of $Fe(CO)_5$ photodissociation products are in agreement with the present results for all but $D[(CO)_3Fe-CO]$, where their estimate of 10 kcal/mol is significantly lower than the value reported here. The theoretically determined bond energies are scattered,[54] but there is reasonable agreement between our unusually low value for $D[Fe-CO]$ and a recent theoretical calculation on Fe(CO) that gives an estimated bond strength of 5 kcal/mol.[9]

Fragment distributions from photolysis of $Fe(CO)_5$ at several wavelengths lead to the estimate that $D[(CO)_2Fe-3CO] \approx 101$ kcal/mol,[17] which implies $D[Fe-2CO] \approx 40$ kcal/mol. These values are in good agreement with the 99 ± 10 and 45 ± 5 kcal/mol values derived here and corroborate that at least one of the two metal–carbonyl bond strengths in $Fe(CO)_2$ is much weaker than the average bond strength.

Nickel Carbonyl. The sum of all three nickel carbonyl bond strengths in $Ni(CO)_3^-$ can be calculated using the literature thermochemistry in Table IV and an equation analogous to eq 14. The result is $D[Ni^--3CO] = 114.3 \pm 1.3$ kcal/mol. Subtraction of $D[(CO)Ni-2CO] = 81.9 \pm 5.8$ kcal/mol obtained in the present study gives $D[Ni-CO] = 32.4 \pm 5.8$ kcal/mol. The paper by CS contains appearance curves for $Ni(CO)_n^-$ fragments formed upon electron bombardment of $Ni(CO)_4$. Again, the AEs have been estimated by Stevens, Feigerle, and Lineberger (SFL),[48] giving the nickel carbonyl bond strengths listed in Table III. These values are in relatively poor agreement with the present results but are within the assigned error limits, except for $D[(CO)_2Ni^--CO]$, which is too low. As for $D[(CO)_3Fe^--CO]$ discussed above, the SFL value for $D[(CO)_2Ni^--CO]$ should be considered a lower limit. The sum of the bond strengths reported by SFL, 95 kcal/mol, is lower than the obligatory sum of 114.3 kcal/mol, consistent with the SFL value for $D[(CO)_2Ni^--CO]$ being too low. The theoretical value available for $D[Ni^--CO]$ is significantly lower than the value derived in this study.[55]

Again, eq 13 can be used in conjunction with bond strengths in the negative ions and metal carbonyl electron affinities[48] to give bond strengths for the neutral species. The higher precision of the EAs in this case allows more precise neutral thermochemistry to be obtained. The results are given in Table III. As for the anions, the results are in generally poor agreement. There are also theoretical calculations available for comparison.[56] Although the sum for $D[Ni-4CO]$ initially obtained from theoretical calculations, 120 kcal/mol, is too low,[56a] the more recent calculated value, 141.5 kcal/mol,[56b] is close to the experimental value of 137.6 ± 1.2 kcal/mol derived from the data in Table IV. This indicates that the more recent theoretical values are not systematically in error. The experimental and theoretical values for $D[(CO)_nNi-CO]$ differ by 4–8 kcal/mol, with the computed values higher for $n = 2$ and 3 and lower for $n = 0$ and 1. The general trend in bond strengths is the same, with $D[(CO)Ni-CO]$ being the strongest bond according to both experiment and theory.

Comparison of CID and EI Results. One question arising from this work pertains to the relative accuracy of metal–carbonyl bond strengths derived from CID and electron impact appearance potential measurements. Both depend on similar threshold measurements, and in both experiments the precision and accuracy of the results decrease significantly as the number of ligands eliminated increases. The CID results are analyzed for quantitative thermochemistry for loss of one or two ligands, and the energetics derived for loss of two ligands are found to be internally consistent with that for two sequential ligand losses. The EI experiments, in contrast, involve loss of up to five ligands, greatly reducing the signal available[57] and increasing the possibility of competitive shifts of the threshold.[46] The EI results for dissociation of two ligands are in good accord with the present results, but the EI results for loss of three or more ligands are not (nor do the two EI results for $D[(CO)Fe^--CO]$ agree with each other). This can be attributed to the inherent uncertainty in determining the thresholds for such high-energy processes. We are also unable to reliably analyze CID data involving loss of more than two ligands with useful precision. A less fundamental difference is that the modeling procedure used for the present data is more reliable than the linear extrapolation used for the EI data, having been calibrated on systems of known thermochemistry (as discussed above). In summary, the two experimental methods are potentially of similar precision, but in the present case the CID results are substantially more reliable. Similar comparisons have been made between CID and appearance potential measurements of the bond strengths in the $Fe(CO)_n^+$ system.[26]

Spin Conservation. The thermochemistry derived above assumes that products are formed in their ground electronic state. With metal carbonyls, this may not always be the case if the reactant and product ions have different spin. For example, addition of CO to $Fe(CO)_4$ is nearly 3 orders of magnitude slower than addition of CO to $Fe(CO)_2$ and $Fe(CO)_3$.[6,58] This is attributed to the spin-forbidden nature of adding a singlet CO to a ground-state triplet[59] $Fe(CO)_4$ to produce ground-state singlet $Fe(CO)_5$. Lewis et al. suggested that the $Fe(CO)_4$–CO bond strength they derived by laser pyrolysis experiments corresponds to forming singlet $Fe(CO)_4$.[13] Theoretical calculations give 15 ± 5[9] and 19.4 kcal/mol[60] for the singlet–triplet gap in $Fe(CO)_4$. However, Seder et al.[58] have suggested that, in the addition of CO to triplet $Fe(CO)_4$, the spin change affects the preexponential factor for the reaction rather than the energetics, and that the activation energy for the reverse reaction is ≤2.5 kcal/mol. Daniel et al. calculated that the singlet–triplet crossing is "allowed with a very low barrier"[60] when spin–orbit coupling is included. ICR studies of the $^{13}CO/^{12}CO$ exchange rates for $Mn(CO)_n^+$ ($n = 1$–5) show that each exchange proceeds efficiently, while kinetic energy release measurements show that there is no excess energy barrier for CO loss for $n = 2$–6.[25] Mn^+ is a septet (and $MnCO^+$ cannot be very low spin[25]) while $Mn(CO)_6^+$ is a singlet. Thus, reactions of metal carbonyls that do not conserve spin are not even necessarily inefficient, nor do they necessarily have a barrier when they are inefficient. These results strongly suggest that the ac-

(54) The theoretical calculations of bond strengths discussed in this paper give 0 K bond energies. We have not corrected these bond strengths due to the lack of necessary information. The effect of temperature is small compared to the error limits of both the experimental and theoretical results.

(55) Bauschlicher, C. W.; Barnes, L. A.; Langhoff, S. R. *Chem. Phys. Lett.* **1988**, *151*, 391–396.

(56) (a) Blomberg, M. R. A.; Brandemark, U. B.; Siegbahn, P. E. M.; Wennerberg, J.; Bauschlicher, C. W. *J. Am. Chem. Soc.* **1988**, *110*, 6650–6655. (b) Blomberg, M. R. A.; Siegbahn, P. E. M.; Lee, T. J.; Rendell, A. P.; Rice, J. A. *J. Chem. Phys.* **1991**, *95*, 5898–5905.

(57) The signal for Fe^- is a factor of 50000 less than the signal for $Fe(CO)_4^-$ in ref 28.

(58) Seder, T. A.; Oudekirk, A. J.; Weitz, E. *J. Chem. Phys.* **1986**, *85*, 1977–1986.

(59) Barton, T. J.; Grinter, R.; Thompson, A. J.; Davies, B.; Poliakoff, M. *J. Chem. Soc., Chem. Commun.* **1977**, 841–842.

(60) Daniel, C.; Bénard, M.; Dedieu, A.; Wiest, R.; Veillard, A. *J. Phys. Chem.* **1984**, *88*, 4805–4811.

tivation energy derived by Lewis et al.[13] corresponds to the adiabatic bond energy for the ground-state species.

The 17-electron species $Ni(CO)_3^-$ is a doublet,[48] while Ni^- is also a doublet.[61] $Ni(CO)^-$ and $Ni(CO)_2^-$ are also probably doublets,[48] which would lead to no difficulties in conserving spin upon dissociation. The situation for iron is more problematic, since $Fe(CO)_4^-$ is again a 17-electron doublet, but Fe^- has a quartet ground state.[47] Thus, one of the carbonyl dissociations either leads to an excited product state or involves a change in spin. In the absence of further information, it is assumed that the products of the CID reactions examined in this work are in their electronic ground states, i.e. that adiabatic dissociation prevails. Note that the presence of the rare gas CID target will tend to break the molecular symmetry and allow nominally spin-forbidden reactions to occur. Also, the excited ions formed by collision with Ar have ca. 10 μs in which to dissociate before reaching the detector. This relatively long time should be sufficient to allow even spin-forbidden processes to occur, particularly since the predissociative ions in question have large amounts of excess energy.

Bond Strength Trends. The successive M–CO bond energies in the iron and nickel carbonyl neutrals and anions do not display any simple homologous trends. Only the extremely weak Fe–CO bond stands out as clearly anomalous. The ground state of Fe(CO) is calculated to be a triplet derived from the $3d^74s$ (^3F) state of Fe,[9] which is 34 kcal/mol above the ground state of Fe. The low bond strength thus correlates with the energy needed to promote the iron atom into a state suitable for bonding. In contrast, promoting Ni from the $3d^84s^2$ ground state to the $3d^94s$ (^3D) state costs only 1 kcal/mol, so the Ni–CO bond is not particularly weak.

The neutral metal–carbonyl bond strengths derived here allow us to evaluate the relationships between the more easily determined mean metal–carbonyl bond strengths[7,8] and the individual bond strengths. Using the data in Table IV, the mean Fe–CO bond strengths in $Fe(CO)_5$ and $Fe(CO)_4^-$ are calculated to be 28.1 and 39.1 kcal/mol, respectively. The mean Ni–CO bond strengths in $Ni(CO)_4$ and $Ni(CO)_3^-$ are 34.4 and 38.1 kcal/mol, respectively. Comparisons with the sequential M–CO values indicate that the average deviation between the mean bond strength and the individual bond strengths is 9–10 kcal/mol for $Fe(CO)_5$ and $Ni(CO)_4$ and 4 kcal/mol for $Fe(CO)_4^-$ and $Ni(CO)_3^-$. Thus, the anionic bond strengths vary less than the neutral bond strengths from the average. If $Fe(CO)_5$ and $Ni(CO)_4$ can be considered typical neutral metal carbonyls, then 9–10 kcal/mol is an estimate of the likely error involved in using a mean bond strength instead of the specific individual bond strength. This substantial deviation highlights the need for additional measurements of the individual bond strengths in metal carbonyl fragments.

Neutral Metal Carbonyl Ionization Potentials. The ionization potentials (IPs) of the neutral metal carbonyl fragments $Fe(CO)_n$ (n = 1–4) and $Ni(CO)_n$ (n = 1–3) have not been directly measured. However, it is possible to estimate the IPs for $Fe(CO)_n$ (n = 1–4) and $Ni(CO)_n$ (n = 1–3) fragments from the neutral bond energies reported here in conjunction with literature thermochemistry. The neutral and cationic metal–carbonyl bond strengths are related through eq 17, which is analogous to eq 16.

$$IP[M(CO)_{n+1}] = IP[M(CO)_n] - D[M(CO)_n^+\text{–CO}] + D[M(CO)_n\text{–CO}] \quad (17)$$

This set of iterative calculations can start from the known IPs of either the bare metal atoms or the 18-electron complexes. Since the IPs of the metal atoms are better known, the calculations are started there. For iron carbonyl, we choose to utilize $(CO)_nFe^+$–CO bond strengths recently derived from CID reactions, which are likely to be the most reliable for reasons discussed in that work.[26] For nickel carbonyl, the $(CO)_nNi^+$–CO bond strengths derived from photoionization threshold measurements by Distefano are used.[23] These cation bond strengths are listed in Tables II and III. Some of the above thermochemistry is nominally at 0 K; small differences between these values and values at 298 K used in the present work are neglected. Somewhat different values can be obtained using other measurements of the cation bond strengths.[22,24]

Table V. Metal Carbonyl Heats of Formation and Ionization Potentials[a]

species	ΔH_f (kcal/mol)	IP (eV)
$Fe(CO)_5$	−173 ± 2[b]	7.93 ± 0.04[c]
		8.03 ± 0.41
$Fe(CO)_4$	−104.5 ± 2.8	7.39 ± 0.41
$Fe(CO)_3$	−55.8 ± 7.6	7.25 ± 0.35
$Fe(CO)_2$	0.2 ± 4.9	6.68 ± 0.24
Fe(CO)	63.9 ± 3.5	6.66 ± 0.17
Fe	99.0 ± 0.2[b]	7.90[b]
$Ni(CO)_4$	−143 ± 1[b]	7.98 ± 0.01[d]
		8.17 ± 0.23
$Ni(CO)_3$	−94.5 ± 1.1	7.69 ± 0.25
$Ni(CO)_2$	−39.0 ± 2.5	7.79 ± 0.22
Ni(CO)	35.1 ± 5.8	7.30 ± 0.29
Ni	102.7 ± 0.7[b]	7.635[b]

[a] Heats of formation are at 298 K; IPs are defined to be at 0 K. [b] Lias, S. G.; Bartmess, J. E.; Liebman, J. F.; Holmes, J. L.; Levin, R. D.; Mallard, W. G. *J. Phys. Chem. Ref. Data* **1988**, *17*, Suppl. 1. [c] Reference 26. [d] Reference 23.

The derived metal carbonyl ionization potentials are given in Table V. The IPs of $Fe(CO)_5$ and $Ni(CO)_4$ are included for comparison in Table V[62] and are in reasonable agreement with the values calculated here, indicating that the calculated IPs are not systematically in error. A similar calculation of ionization potentials has been carried out previously using earlier values for the neutral iron carbonyl bond strengths.[24]

For iron, the first carbonyl ligand greatly decreases the ionization potential, while additional carbonyl ligands increase the IP. The low IP of Fe(CO) is a reflection of D[Fe–CO] being significantly lower than D[Fe^+–CO]. For nickel, the most noteworthy finding is that the IP of Ni(CO) is significantly lower than the others. The IPs of $Ni(CO)_n$ (n = 1–4) are 0.05–0.62 eV higher than the IPs of the isoelectronic $Fe(CO)_{n+1}$ ions, while IP[Ni] is 1.09 eV higher than the isoelectronic IP[Fe(CO)]. This also highlights the anomalously low Fe–CO bond strength.

Since the IPs of the neutral iron and nickel carbonyl fragments have not been directly determined, it is not currently possible to derive the neutral metal–carbonyl bond strengths from the cation data using eq 17. Independent measurements of these ionization potentials would be of great value as a check on the currently available thermochemistry.

Related Metal–Ligand Bond Strengths. Knowledge of metal–carbonyl bond strengths also allows thermochemical information for other ligands to be derived from studies of ligand exchange reactions.[63-66] These can be used to determine the relative ordering of metal–ligand bond strengths, since, for gas-phase ligand substitution reactions to be efficient, the reaction must be exothermic or thermoneutral.[67] Bimolecular reaction rates for a number of gas-phase ligand substitution reactions involving $Fe(CO)_2^-$,[65,68] $Fe(CO)_3^-$,[63,68] $Fe(CO)_4^-$,[64,66] and $Ni(CO)_3^-$[66] have

(61) Corderman, R. R.; Engelking, P. C.; Lineberger, W. C. *J. Chem. Phys.* **1979**, *70*, 4474–4480.

(62) IP[$Ni(CO)_4$] is taken from ref 23, and IP[$Fe(CO)_5$] is taken to be the average of previous determinations given in ref 26.

(63) Addition of CO to $Fe(CO)_3^-$ has been reported previously in: McDonald, R. N.; Chowdhury, A. K.; Schell, P. L. *J. Am. Chem. Soc.* **1984**, *106*, 6095–6096.

(64) McDonald, R. N.; Schell, P. L. *Organometallics* **1988**, *7*, 1820–1827.

(65) McDonald, R. N.; Chowdhury, A. K.; Jones, M. T. *J. Am. Chem. Soc.* **1986**, *108*, 3105–3107.

(66) Pan, Y. H.; Ridge, D. P. *J. Am. Chem. Soc.* **1989**, *111*, 1150–1151. Pan, Y. H.; Ridge, D. P. *J. Am. Chem. Soc.*, submitted for publication, and references cited therein.

(67) Reaction at 10% of the ion–neutral collision rate can be considered efficient for this purpose. If a ligand substitution is inefficient, it is not necessarily endothermic, since there may be a barrier to reaction. Indeed, the strong correlations between reactivity and ligand electron affinity that have been noted recently suggest a mechanism involving initial electron transfer from the metal complex to the ligand, implying the existence of barriers for reactants with low electron affinities. See ref 66 and: Jones, M. T.; McDonald, R. N.; Schell, P. L.; Ali, M. H. *J. Am. Chem. Soc.* **1989**, *111*, 5983–5992.

been reported recently. Observation of reaction 18 implies

$$(CO)_nM^- + L \rightarrow (CO)_{n-m}ML^- + mCO \quad (18)$$

$D[(CO)_{n-m}M^- - L] \geq D[(CO)_{n-m}M^- - mCO]$. Thermochemical results that can be derived from such reactions include $D[(CO)_3Fe^- - L] \geq 41.7 \pm 2.5$ kcal/mol for L = SO_2 and $(CF_3)_2CO$;[63] $D[(CO)_2Fe^- - C_2H_2] \geq 42.4 \pm 3.5$ kcal/mol,[63] $D[(CO)_2Fe^- - L] \geq 84.1 \pm 4.3$ kcal/mol for L = 1,3- and 1,4-dinitrobenzene, 1,4-benzoquinone, and tetracyanoethylene; $D[(CO)Fe^- - CS_2] \geq 78.2 \pm 4.9$ kcal/mol;[68] $D[Fe^- - CS_2] \geq 111.8 \pm 8.0$ kcal/mol;[68] $D[(CO)_2Ni^- - L] \geq 38.5 \pm 2.3$ kcal/mol for L = nitrobenzene; $D[(CO)Ni^- - L] \geq 81.9 \pm 5.8$ kcal/mol for L = 1,4-benzoquinone and tetracyanoethylene; and $D[Ni^- - L] \geq 114.3 \pm 1.3$ kcal/mol for 1,2- and 1,4-bromonitrobenzene.[66] Further thermochemical implications for various aromatic compounds can be made from the data in ref 66.

Another method for deriving thermochemistry is to combine the measured enthalpy of disruption[7] of organometallic species containing metal carbonyl fragments, eq 19, with the metal-

$$\Delta H_{disr}[M(CO)_nL_m] = \Delta H_f(M) + n\Delta H_f(CO) + m\Delta H_f(L) - \Delta H_f[M(CO)_nL_m] \quad (19)$$

carbonyl bond strengths to derive bond strengths for the other ligands. The results derived using this procedure include $D[(CO)_4Fe-C_2H_4] = 36.5 \pm 3.6$ kcal/mol,[69] $D[(CO)_3Fe-C_4H_6] = 56.0 \pm 8$ kcal/mol,[69] $D[(CO)Fe-2(C_4H_6)] = 103.4 \pm 5$ kcal/mol,[69] $D[(CO)Fe-2(C_6H_8)] = 109.6 \pm 5$ kcal/mol,[69] and $D[(CO)_3Fe-C_8H_8] = 50.9 \pm 8.4$ kcal/mol[70] (C_4H_6 = 1,3-butadiene, C_6H_8 = cyclohexa-1,3-diene, and C_8H_8 = 1,3,5,7-cyclooctatetraene). Similar analyses have been carried out previously using mean metal-carbonyl bond strengths instead of the individual values.[7,69,70] These calculations give consistently lower metal-ligand bond strengths. The present values indicate that bonds from iron to one, two, or four alkene groups are slightly weaker than bonds to the corresponding number of carbonyl ligands. No analogous enthalpies of disruption are available for compounds containing nickel carbonyl fragments, but studies of substitution equilibria[71] indicate that nickel-olefin bond strengths are in the 25-42 kcal/mol range, similar to the values encountered in the iron-containing systems.

The individual metal-carbonyl bond strengths can be used with heats of formation given in Table IV to derive values for the heats of formation of the metal carbonyl fragments. The heats of formation of $Fe(CO)_n^-$ (n = 1-3) are calculated iteratively starting with the heat of formation of Fe. $\Delta H_f(Fe(CO)_4$ is derived from the heat of formation of $Fe(CO)_5$ and $D[(CO)_4Fe-CO]$. The results are given in Table V and may be useful for deriving additional metal-ligand bond energies when further calorimetrically determined heats of formation for $Fe(CO)_n$- and $Ni(CO)_n$-containing species become available.

Conclusions

Energy-resolved collision-induced dissociation has been used to determine the metal-carbonyl bond energies in $Fe(CO)_n^-$ (n = 1-4) and $Ni(CO)_n^-$ (n = 2, 3). These can be combined with literature thermochemistry to give $D[Ni^- - CO]$, ionization potentials and heats of formation for the neutral iron and nickel carbonyls and, perhaps most significantly, metal-carbonyl bond strengths in the neutral fragments. These results are compared to previous experimental and theoretical estimates. The results suggest that the thermochemistry determined from loss of one or two CO ligands is essentially unaffected by electron detachment, competitive shifts, or reaction barriers in excess of the dissociation endothermicities. The present results can be used to derive thermodynamic data for other organometallic species which contain metal carbonyl fragments, in particular species where one to four carbonyl ligands are replaced with alkene ligands.

The sequential M-CO bond strengths in the iron and nickel carbonyls deviate from the mean value by an average of up to 10 kcal/mol, emphasizing the importance of measuring sequential rather than average bond strengths. The deviation from the mean is particularly large for $D[Fe-CO]$, which is exceptionally low (8.1 ± 3.5 kcal/mol), in agreement with recent theoretical predictions. Further work in this laboratory will provide bond strength determinations for other metal carbonyls that should make any correlations between metal-carbonyl bond strengths and electron count, charge state, or number of ligands more apparent.

Acknowledgment. This work was supported by the Department of Energy, Office of Basic Energy Science. We thank Drs. C. W. Bauschlicher and T. J. Lee, and R. H. Schultz, K. C. Crellin, and Prof. P. B. Armentrout, for sending their results prior to publication.

(68) Gregor, I. K. *Inorg. Chim. Acta* **1990**, *176*, 19-22.
(69) Brown, D. L. S.; Connor, J. A.; Leung, M. L.; Paz-Andrade, M. I.; Skinner, H. A. *J. Organomet. Chem.* **1976**, *110*, 79-89.
(70) Connor, J. A.; Demain, C. P.; Skinner, H. A.; Zafarini-Moattar, M. T. *J. Organomet. Chem.* **1979**, *170*, 117-130.
(71) Tolman, C. A. *J. Am. Chem. Soc.* **1974**, *96*, 2780-2789.

Structure and Energetics of Clean and Hydrogenated Diamond (100) Surfaces by Molecular Mechanics

Yuemei L. Yang and Mark P. D'Evelyn*

Contribution from the Department of Chemistry and Rice Quantum Institute, Rice University, Houston, Texas 77251-1892. *Received August 7, 1991*

Abstract: The molecular mechanics (MM3) method has been applied to the clean and hydrogenated surfaces of diamond (100). Periodic boundary conditions are incorporated into the computational algorithm, permitting calculations comparable in size to modest-sized clusters but without complications from edge effects. The atomic structure and energetics of the clean (100)-(2×1), monohydride (100)-(2×1):H, full dihydride (100)-(1×1):2H, and intermediate dihydride (100)-(3×1):1.33H surfaces have been determined. Pairs of surface carbon atoms form symmetric dimers on the reconstructed diamond (100)-(2×1), (2×1):H, and (3×1):1.33H surfaces, with dimer bond lengths of 1.46, 1.63, and 1.59 Å, respectively, corresponding to strained double or single bonds. The full (1×1):2H dihydride, with two hydrogen atoms per surface carbon atom, is highly strained due to H-H repulsions, causing a reduction of the H-C-H bond angle and twisting about the surface normal, and is predicted to be thermodynamically unstable with respect to dehydrogenation to the monohydride. Some important gas-surface reactions involving hydrogen and the diamond (100) surface are discussed in light of the derived energetics.

Phenomenal progress has been made over the past few years in the low-pressure growth of diamond films by chemical vapor deposition (CVD).[1] Hydrogen atoms are known to enhance the growth of diamond while suppressing graphite growth in the CVD

0002-7863/92/1514-2796$03.00/0